JOURNAL OF Materials CHEMISTRY

Nonlinear absorption properties of some 1,4,8,11,15,18,22,25-octaalkylphthalocyanines and their metallated derivatives

Aurélien Auger,[a] Werner J. Blau,*[b] Paul M. Burnham,[a] Isabelle Chambrier,[a] Michael J. Cook,*[a] Benjamin Isare,[a] Fabien Nekelson[a] and Sean M. O'Flaherty[b]

[a] *Wolfson Materials and Catalysis Centre, School of Chemical Sciences and Pharmacy, University of East Anglia, Norwich, UK NR4 7TJ*
[b] *Materials Ireland Polymer Research Centre, Department of Physics, Trinity College Dublin, Dublin 2, Republic of Ireland*

Received 7th January 2003, Accepted 6th March 2003
First published as an Advance Article on the web 26th March 2003

The third-order nonlinear optical properties of a series of 15 unmetallated and metallated 1,4,8,11,15,18,22,25-octaalkylphthalocyanines have been investigated. The palladium-metallated compound is the strongest nonlinear absorber of the series, but, due to its comparatively high linear absorption coefficient, it exhibits a relatively low ratio of excited- to ground-state absorption cross-sections (κ) when compared to the other compounds. The highest values for κ were found for derivatives metallated with indium and lead. The nickel-metallated compounds are the weakest nonlinear absorbers, indicating that they are unsuitable as potential materials for practical passive optical limiters. Phenomenologically, the data for κ and the saturation energy density (F_{sat}) were found to follow trends dependent upon the linear absorption coefficient. This may have some implications for the design of phthalocyanines for nonlinear optical applications.

1 Introduction

Optical limiters are materials that exhibit decreased transmission of light as incident light intensity is increased. Such a property, when applied to the attenuation of incident light intensity from laser pulses,[1] for example, is recognised to have potential applications for the protection of human eyes and optically sensitive equipment. The phenomenon is a consequence of one or more nonlinear absorption processes, among which reverse saturable absorption (RSA) is recognised to be particularly important.[2] During RSA, nonlinear absorption arises through further electronic excitation within a molecule already in an electronically excited state. Compounds exhibiting RSA as a result of $T_1 \rightarrow T_2$ excitation are most efficient as optical limiters when (i) there is efficient intersystem crossing from the S_1 excited state to T_1, (ii) the T_1 state is long lived and (iii) the $T_1 \rightarrow T_2$ transition has a large absorption cross-section. Phthalocyanines and their derivatives are attractive candidates for optical limiting[3,4] because the ring system exhibits a number of the appropriate photophysical properties. Furthermore, there is potential to tune the desirable properties through the incorporation of different elements into the central cavity and/or substitution of the ring system.[5–8] Metallated phthalocyanines shown to possess useful optical limiting behaviour include those containing aluminium,[9] indium,[10] silicon,[11] vanadium,[12] lead,[13] titanium,[14] nickel,[15] gallium,[16] tin[17] and various lanthanides.[18] In previous studies, compounds have generally been substituted to promote solubility. Ideally, substituents should also minimise cofacial aggregation, because this introduces further relaxation pathways which serve to shorten excited-state lifetimes. Thus derivatives bearing one or two axial ligands at the metal (or metalloid) centre, as in the majority of metallated phthalocyanines listed above, have received considerable attention.

Previous work from one of our laboratories[19] has demonstrated that eight straight alkyl chains located at the 1, 4, 8, 11, 15, 18, 22 and 25 sites of the phthalocyanine nucleus promote solubility in most aprotic organic solvents, particularly when the chains contain an even number of carbon atoms;[20] they also have a beneficial effect in reducing aggregation.[20] *iso*-Pentyl groups in these sites cause distortion of the ring from planarity in the metal-free phthalocyanine and also show advantageous solubilising effects.[21] The present paper reports a systematic study and comparison of the nonlinear absorption properties of a series of 15 octaalkyl-substituted compounds, covering a range of 7 metal centres, as well as the metal-free analogues. Measurements have been undertaken using the Z-scan method to investigate the nonlinear excited-state behaviour of the compounds and provide an insight into the effects of structural modification on the nonlinear optical response of phthalocyanine moieties.

2 Experimental

2.1 Characterisation

^{1}H NMR spectra were recorded at 270 MHz using a JEOL EX 270 spectrometer, at 300 MHz on a Varian Gemini 2000 spectrometer or at 400 MHz on a Varian Unity$_{plus}$ spectrometer. ^{13}C NMR spectra were measured on the same equipment at 67.5, 75 and 100 MHz, respectively. Tetramethylsilane was used as the internal standard and the positions of the peaks are reported in ppm. The splittings of the signals are described as singlets (s), doublets (d), triplets (t), quartets (q), quintets (qn), broad (br) or multiplets (m). The UV-Vis spectra were recorded using a Hitachi U-3000-X spectrophotometer. Low resolution matrix-assisted laser desorption ionisation (MALDI) mass spectra were obtained using a dithranol matrix at the University of Manchester, UK. Elemental analysis was carried out by the microanalytical service provided at the University of East Anglia by Mr A. W. Saunders.

Solvents were HPLC grade or better. They were not specifically dried unless otherwise stated. Petrol refers to light petroleum (b.p. 40–60 °C).

Silica gel (Merck grade 7734) was used in chromatographic separations. TLC was performed using Merck 5554 silica gel on aluminium sheets.

 DOI: 10.1039/b300199g

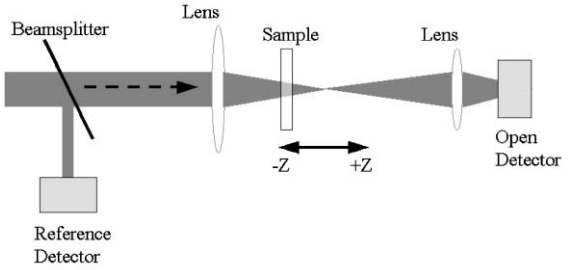

Fig. 1 Schematic diagram of the open-aperture Z-scan apparatus.

2.2 NLO measurements

The open-aperture Z-scan technique[22] measures the total optical transmittance through a sample as a function of incident laser intensity while the sample is gradually moved through the focus of a lens (along the z axis). The set-up is shown schematically in Fig. 1. Absorption coefficients were calculated by the fitting theory previously reported.[22] The normalised transmittance as a function of position z (see Fig. 3), $T_{\mathrm{norm}}(z)$, is given by

$$T_{\mathrm{norm}}(z) = \frac{\ln[1+q_0(z)]}{q_0(z)} \quad (1)$$

where $q_0(z)$ is given by

$$q_0(z) = \frac{q_{00}}{1+\left(\frac{z}{z_0}\right)^2} \quad (2)$$

z_0 is the diffraction length of the beam and $q_{00} = \beta_{\mathrm{eff}} I_0 L_{\mathrm{eff}}$, where $L_{\mathrm{eff}} = [1 - \exp(-\alpha_0 L)]/\alpha_0$, β_{eff} is the effective intensity-dependent nonlinear absorption coefficient and I_0 is the intensity of the light at focus. L_{eff} is known as the effective length of the sample and is defined in terms of the linear absorption coefficient, α_0, and the true optical path length through the sample, L.

The imaginary third-order optical susceptibility, $\mathrm{Im}\{\chi^{(3)}\}$, is directly related to the intensity-dependent absorption coefficient, β_I, and is expressed as

$$\mathrm{Im}\{\chi^{(3)}\} = \frac{n_0^2 \varepsilon_0 c \lambda \beta_I}{2\pi} \quad (3)$$

where n_0 is the linear refractive index, ε_0 is the permittivity of free space, c is the speed of light and λ is the wavelength of the incident light. This expression is strictly only true for constant β_I over incident intensities, corresponding to the physical situation where third-order effects are the only contribution to the nonlinear response. The relationship between $\mathrm{Im}\{\chi^{(3)}\}$ and the imaginary second-order molecular hyperpolarisability, $\mathrm{Im}\{\gamma\}$, is defined as

$$\mathrm{Im}\{\gamma\} = \frac{\mathrm{Im}\{\chi^{(3)}\}}{f^4 c_{\mathrm{mol}} N_{\mathrm{A}}} \quad (4)$$

where $f = (n_0^2 + 2)/3$ is the Lorentz local field enhancement factor, n_0 is the linear refractive index of the sample, c_{mol} is the molar concentration and N_{A} is Avogadro's number.

All experiments described in this study were performed using 6 ns pulses from a Q-switched Nd : YAG laser. The beam was spatially filtered to remove the higher order modes and tightly focused with a 9 cm focal length lens. The laser was operated at its second harmonic, 532 nm, with a pulse repetition rate of 10 Hz. All samples were prepared by dissolving the compound in a suitable common organic solvent (toluene or THF) at 1.0 g L^{-1}, followed by gentle agitation for $\approx$20 min in a low power (60 W) sonic bath to ensure complete and uniform dispersal. All measurements were performed in quartz cells with a 1 mm through path length.

2.3 Materials

The synthesis and characterisation of **1**, **2**,[23] **3**,[21] **4**, **5**,[24] **6** and **7**[20] have been described elsewhere.

Preparation of 1,4,8,11,15,18,22,25-octakis(3-methylbutyl)-phthalocyaninatozinc(II), 8. In a typical procedure, 1,4,8,11,15,18,22,25-octakis(3-methylbutyl)phthalocyanine[23] (**3**; 320 mg, 0.28 mmol) was dissolved in pentan-1-ol (10 ml) and heated to reflux. Excess metal salt, zinc(II) acetate (0.2 mg, 0.91 mmol), was added and reflux was continued for 4 h. After the reaction mixture had cooled, methanol (10 ml) was added and the precipitate collected and chromatographed over silica gel (eluent: petrol–THF 2 : 1), collecting the green fraction, which was recrystallised from THF–methanol to give **8** (270 mg, 80%) as blue needles. M.p. > 300 °C. Found: C, 74.91; H, 8.4; N, 9.4; $C_{72}H_{96}N_8Zn{\cdot}CH_3OH$ requires: C, 74.94; H, 8.53; N, 9.58%. δ_{H} (400 MHz, $CDCl_3$) 7.88 (8H, s), 4.59 (16H, t), 2.02 (16H, m), 1.86 (8H, m), 1.03 (48H, d). λ_{max} (abs.) 703 nm (THF), ε = 2.2 × 10^5 M^{-1} cm^{-1}.

Preparation of 1,4,8,11,15,18,22,25-octakis(3-methylbutyl)-phthalocyaninatocopper(II), 9. 3,6-Bis(3-methylbutyl)phthalonitrile[23] (1.5 g, 5.6 mmol) in pentan-1-ol (16 ml) was brought to reflux and copper(II) acetate (0.30 g, 1.68 mmol) was added. After addition of DBU (0.60 g, 3.92 mmol), the reaction mixture turned green and reflux was continued for 12 h. The mixture was allowed to cool and the solvents were removed under reduced pressure. The resulting precipitate was washed onto a filter with methanol. The crude product was purified by column chromatography over silica (eluent: petrol–DCM 4 : 1). Recrystallisation from THF–acetone afforded **9** (320 mg, 22%) as a blue solid. M.p. > 300 °C. Found: C, 75.7; H, 8.6; N, 9.6; $C_{72}H_{96}N_8Cu$ requires: C, 76.05; H, 8.2; N, 9.9%. λ_{max} (abs.) 705 nm (THF), ε = 0.6 × 10^5 M^{-1} cm^{-1}.

Preparation of 1,4,8,11,15,18,22,25-octakis(hexyl)phthalocyaninatopalladium(II), 10. Compound **10** was prepared as described above for compound **8**, using 1,4,8,11,15,18,22,25-octakis(hexyl)phthalocyanine (**1**; 166 mg, 0.14 mmol) and palladium(II) acetate (0.20 g, 0.89 mmol) as the metal salt. The title compound was obtained as a blue powder (140 mg, 77%). Found: C, 74.47; H, 8.85; N, 8.27; $C_{80}H_{112}N_8Pd$ requires: C, 74.35; H, 8.74; N, 8.67%. δ_{H} (300 MHz, C_6D_6) 7.28 (8H, s), 4.01 (16H, t), 1.83 (16H, m), 1.33 (16H, m), 0.98 (32H, m), 0.52 (24H, t). λ_{max} (abs.) 690 nm (cyclohexane), ε = 1.0 × 10^5 M^{-1} cm^{-1}. MALDI-MS: isotopic cluster at 1291 (M^+, 100%).

Preparation of 1,4,8,11,15,18,22,25-octakis(hexyl)phthalocyaninatolead(II), 11. Compound **11** was prepared as described above for compound **8**, using **1** (120 mg, 0.1 mmol) and lead(II) acetate in excess (75 mg) as the metal salt. The title compound was purified by column chromatography over silica gel (eluent: petrol–triethylamine 99 : 1) and obtained as green needles (67 mg, 48%). M.p. 144–146 °C. Found: C, 69.19; H, 8.17; N, 7.98; $C_{80}H_{112}N_8Pb$ requires: C, 69.02; H, 8.05; N, 8.05%. δ_{H} (270 MHz, C_6D_6) 7.88 (8H, s), 4.98–4.88 (8H, m), 4.67–4.57 (8H, m), 2.35 (16H, qn), 1.74 (16H, qn), 1.45–1.22 (32H, m), 0.83 (24H, t). MALDI-MS: isotopic cluster at 1393 (M^+, 100%). λ_{max} (abs.) 746 nm (toluene), ε = 1.4 × 10^5 M^{-1} cm^{-1}.

Preparation of 1,4,8,11,15,18,22,25-octakis(3-methylbutyl)-phthalocyaninatolead(II), 12. Compound **12** was prepared as described above for compound **8**, using **3** (320 mg, 0.29 mmol) and lead(II) acetate (0.10g, 0.26 mmol) as the metal salt. The title compound was obtained as green needles (250 mg, 65%). M.p. 256 °C. Found: C, 66.95; H, 7.59; N, 8.24; $C_{72}H_{96}N_8Pb$

requires: C, 67.52; H, 7.55; N, 8.75%. δ_H (400 MHz, $CDCl_3$) 7.83 (8H, s), 4.92 (8H, m), 4.63 (8H, m), 2.14 (16H, m), 2.0 (8H, m), 1.06 (48H, d). λ_{max} (abs.) 744 nm (THF), $\varepsilon = 1.6 \times 10^5$ M^{-1} cm^{-1}.

Preparation of chloro[1,4,8,11,15,18,22,25-octakis(hexyl)-phthalocyaninato]indium(III), 13. 1 (120 mg, 0.1 mmol) was dissolved in pentan-1-ol (7 ml) and heated to reflux. Excess indium(III) chloride (80 mg) was added and reflux was continued for 2 h. The solvent was removed under reduced pressure and the resultant green residue chromatographed over silica gel, first eluting with petrol to remove a residual amount of the starting material and then with petrol–THF (19 : 1), collecting the first green fraction, which was recrystallised from THF–acetone to give **13** (58 mg, 43%) as fine green needles. M.p. 110–112 °C. Found: C, 72.27; H, 8.32; N, 8.17; $C_{80}H_{112}N_8InCl$ requires: C, 71.92; H, 8.45; N, 8.39%. δ_H (270 MHz, C_6D_6, 50 °C) 7.92 (8H, s), 4.84–4.62 (16H, m), 2.35–2.24 (16H, m), 1.84–1.70 (16H, m), 1.48–1.22 (32H, m), 0.82 (24H, t). δ_C (75 MHz, $CDCl_3$) 153.3, 139.5, 134.9, 131.2, 32.6, 32.1, 30.5, 28.9, 22.6, 14.0. MALDI-MS: isotopic cluster at 1336 (M^+, 100%). λ_{max} (abs.) 729 nm (toluene), $\varepsilon = 2.2 \times 10^5$ M^{-1} cm^{-1}.

Preparation of 4-fluorophenyl[1,4,8,11,15,18,22,25-octakis-(hexyl)phthalocyaninato]indium(III), 14. 1-Bromo-4-fluorobenzene (1.14 g, 6.5 mmol) in dry THF (10 ml) was added dropwise to a stirred mixture of magnesium turnings (200 mg, 8.2 mmol), 1,2-dibromoethane (4 drops) and iodine (1 crystal) in dry THF (15 ml) under an atmosphere of argon. Once the addition was complete, the reaction mixture was kept at reflux for 90 min before being allowed to cool to room temperature. A portion of the solution (3 ml) containing the Grignard reagent 4-fluorophenylmagnesium bromide was added to a solution of **13** (100 mg, 0.07 mmol) in dry THF (2 ml) and stirred at room temperature under an atmosphere of argon. After 10 min, the reaction mixture was concentrated under reduced pressure, triturated with methanol (2 × 10 ml), filtered and the solid purified by column chromatography over silica gel, eluting with petrol–DCM (1/1). The first green fraction was collected and recrystallised from THF–methanol to give **14** (73 mg, 75%) as blue–green needles. M.p. 127–129 °C. Found: C, 73.00; H, 8.42; N, 7.70; $C_{86}H_{116}N_8InF$ requires: C, 74.01; H, 8.38; N, 8.03%. δ_H (400 MHz, $CDCl_3$) 7.87 (8H, s), 5.60 (2H, t), 4.61–4.54 (8H, m), 4.41–4.34 (8H, m), 3.88 (2H, t), 2.23–2.03 (16H, m), 1.56–1.45 (16H, m), 1.30–1.14 (32H, m), 0.74 (24H, t). δ_C (100 MHz, $CDCl_3$) 154.0, 139.4, 135.6 (d, *J* 6.1), 135.2, 131.1, 113.6 (d, *J* 19.0 Hz), 33.0, 32.4, 30.9, 29.1, 22.9, 14.3. MALDI-MS: isotopic cluster at 1395 (M^+, 100%). λ_{max} (abs.) 728 nm (THF), $\varepsilon = 2.2 \times 10^5$ M^{-1} cm^{-1}.

Preparation of dihydroxy[1,4,8,11,15,18,22,25-octakis(hexyl)-phthalocyaninato]silicon, 15. 1 (200 mg, 0.17 mmol) and tri-*n*-butylamine (20 ml) were stirred in freshly distilled dry DCM (18 ml) under argon. When all the starting materials had dissolved, trichlorosilane (1.2 ml, 12 mmol) was added *via* a plastic syringe directly into the solution. The dark green solution was stirred for 4 h. TLC analysis (eluent: cyclohexane) showed the completion of the reaction after 4 h. The mixture was then poured cautiously into water (120 ml) and triethylamine (70 ml) was added slowly. The green precipitate was filtered out and washed with DCM until the washings were almost clear. The organic phase was separated, washed with 20% aq. HCl (5 × 100 ml), water (3 × 100 ml), brine (2 × 100 ml) and dried over $MgSO_4$.The drying agent was removed by filtration and the solvent was evaporated under vacuum. The dark blue residue was chromatographed over silica (eluent: cyclohexane–toluene 2 : 1 then 1 : 2). After removing the solvent under reduced pressure, **15** was obtained (180 mg, 87%) as a thick dark blue oil. Found: C, 76.94; H, 9.33; N, 8.43; $C_{80}H_{114}N_8O_2Si$ requires: C, 76.99; H, 9.21; N, 8.98%. δ_H (400 MHz, C_6D_6) 7.91 (8H, s), 4.70 (16H, t), 2.30 (16H, qn), 1.75 (16H, qn), 1.38 (32H, m) 0.88 (24H, t), −5.74 (2H, br s). δ_C (75 MHz, C_6D_6) 147.96, 138.41, 133.44, 130.14, 31.88, 31.27, 29.80, 28.31, 21.78, 12.96. MALDI-MS isotopic clusters at 1248 (20%, M^+) and 1231 (100%, M − H_2O). λ_{max} (abs.) 703.5 nm (THF), $\varepsilon = 2.4 \times 10^5$ M^{-1} cm^{-1}.

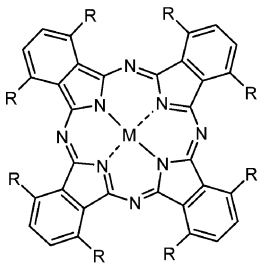

1	M=H,H	R=*n*-C_6H_{13}
2	M=H,H	R=*n*-$C_{10}H_{21}$
3	M=H,H	R=*i*-C_5H_{11}
4	M=Ni	R=*n*-C_6H_{13}
5	M=Ni	R=*n*-$C_{10}H_{21}$
6	M=Zn	R=*n*-C_6H_{13}
7	M=Zn	R=*n*-$C_{10}H_{21}$
8	M=Zn	R=*i*-C_5H_{11}
9	M=Cu	R=*i*-C_5H_{11}
10	M=Pd	R=*n*-C_6H_{13}
11	M=Pb	R=*n*-C_6H_{13}
12	M=Pb	R=*i*-C_5H_{11}
13	M=InCl	R=*n*-C_6H_{13}
14	M=InArF	R=*n*-C_6H_{13}
15	M=$Si(OH)_2$	R=*n*-C_6H_{13}

3 Results and discussion

3.1 Preparation of materials

The synthesis and characterisation of **1**–**7** have been described elsewhere[20,21,23,24] and the synthetic protocols devised earlier were applied within the syntheses of the novel compounds **8**–**15**. Thus, octaalkylphthalocyanine derivatives were synthesised using the corresponding 3,6-dialkylphthalonitriles[23] as precursors. The latter were cyclotetramerised under basic conditions to afford the metal-free phthalocyanines.[23] Metallated derivatives were prepared either by direct cyclotetramerisation of the phthalonitriles in the presence of the appropriate metal salt, as in the case of **9**, or by metal ion insertion into the metal-free analogue, which provided access to **8** and **10**–**12**. The novel chloroindium derivative **13** was obtained by reacting the metal-free phthalocyanine with indium trichloride in pentanol. This was then converted into the 4-fluorophenylindium derivative **14** using Grignard chemistry *via* procedures applied to related compounds by Hanack and Heckmann.[25] The dihydroxysilicon phthalocyanine **15** was prepared from the corresponding metal-free phthalocyanine using the general procedure developed by Kenney *et al.*[26]

3.2 Optical limiting measurements

The linear absorption spectra of phthalocyanine compounds have two main features: a Q band in the region of 700 nm and a B band in the region of 350 nm. These materials have a window between these two absorption bands with high linear transmittance, making them attractive as limiters of visible light ($\lambda \approx$ 420–650 nm). The location (wavelength) of the peak of the Q band (lowest energy transition) is quoted for each of compounds **1**–**15** in Table 1.

All open-aperture Z-scans performed in this study exhibited a reduction in the transmission about the focus of the lens. This is typical of an induced positive nonlinear absorption of the incident light; in this case, attributed to reverse saturable excited-state absorption. All open-aperture Z-scan datasets were fitted using the method of least squares regression with eqn. 1 and eqn. 2. The beam waist radius w_0 and the nonlinear absorption coefficient β_I were treated as free parameters in the fit, and all fits typically converged with R^2 values in excess of 0.99. A sample of a typical open-aperture Z-scan spectrum with normalised transmission plotted as a function of sample position z is depicted in Fig. 2 for compound **10** under incident focal intensity of 0.36 GW cm^{-2}. It was noticed that the nonlinear absorption coefficient β_I, in all cases, was not stationary with respect to the on-focus intensity. In Fig. 3, plots

Table 1 Linear optical properties, calculated nonlinear optical coefficients and optical limiting parameters for compounds **1–15**; measured in toluene, except where otherwise indicated

	Central atom	Alkyl chain	c/g L^{-1}	α_0/cm^{-1}	λ_{max}/nm	I_0/GW cm^{-2}	β_I/cm W^{-1}	Im$\{\chi^{(3)}_{eff}\}$/esu	Im$\{\gamma_{eff}\}$/esu	F_{sat}/J cm^{-2}	κ (σ_{ex}/σ_0)
1	H_2	Hexyl	1.0	0.94	733	0.5	(1.8 ± 0.3) × 10^{-8}	(6.6 ± 1.3) × 10^{-12}	(3.6 ± 0.7) × 10^{-32}	16.8 ± 0.6	14.5 ± 0.3
2	H_2	Decyl	1.0	0.83	730	0.5	(1.5 ± 0.3) × 10^{-8}	(5.8 ± 1.1) × 10^{-12}	(4.3 ± 0.8) × 10^{-33}	20.2 ± 1.0	14.4 ± 0.5
3	H_2	Isopentyl	1.0	0.94	731	0.5	(1.6 ± 0.3) × 10^{-8}	(5.9 ± 1.1) × 10^{-12}	(3.0 ± 0.6) × 10^{-33}	14.4 ± 0.5	11.3 ± 0.3
4	Ni	Hexyl	1.0	1.05	702	0.5	(1.6 ± 0.3) × 10^{-9}	(5.9 ± 1.1) × 10^{-13}	(3.4 ± 0.6) × 10^{-34}	18 ± 3	2.4 ± 0.2
5	Ni	Decyl	1.0	0.94	702	0.5	(1.5 ± 0.3) × 10^{-9}	(5.5 ± 1.1) × 10^{-13}	(4.2 ± 0.8) × 10^{-34}	13.3 ± 2.0	2.1 ± 0.1
6	Zn	Hexyl	1.0	1.17	705	0.5	(4.0 ± 0.8) × 10^{-8}	(1.5 ± 0.3) × 10^{-11}	(8.6 ± 1.7) × 10^{-33}	7.1 ± 0.3	11.4 ± 0.3
7	Zn	Decyl	1.0	1.17	705	0.5	(2.4 ± 0.4) × 10^{-8}	(9.1 ± 1.8) × 10^{-12}	(6.9 ± 1.3) × 10^{-33}	13.6 ± 0.5	11.7 ± 0.3
8	Zn	Isopentyl	1.0	1.05	703	0.5	(4.0 ± 0.8) × 10^{-8}	(1.5 ± 0.3) × 10^{-11}	(7.9 ± 1.5) × 10^{-33}	6.6 ± 0.2	12.2 ± 0.3
9	Cu	Isopentyl	1.0	1.63	705	0.5	(6.4 ± 1.0) × 10^{-8}	(2.4 ± 0.4) × 10^{-11}	(1.3 ± 0.2) × 10^{-32}	4.6 ± 0.1	8.8 ± 0.1
10	Pd	Hexyl	1.0	2.60	687	0.5	(9.6 ± 1.9) × 10^{-8}	(3.6 ± 0.7) × 10^{-11}	(2.1 ± 0.4) × 10^{-32}	2.1 ± 0.1	5.9 ± 0.1
11	Pb	Hexyl	1.0	0.83	741	0.5	(2.9 ± 0.6) × 10^{-8}	(1.1 ± 0.2) × 10^{-11}	(7.0 ± 1.4) × 10^{-33}	9.8 ± 0.3	16.1 ± 0.3
12	Pb	Isopentyl	1.0	1.06	744	0.5	(4.6 ± 0.8) × 10^{-8}	(1.7 ± 0.3) × 10^{-11}	(9.2 ± 1.6) × 10^{-33}	7.1 ± 0.2	14.2 ± 0.2
13	InCl	Hexyl	1.0	0.93	730	0.5	(3.2 ± 0.6) × 10^{-8}	(1.2 ± 0.2) × 10^{-11}	(7.3 ± 1.4) × 10^{-33}	10.1 ± 0.5	16.1 ± 0.3
14	InArF	Hexyl	1.0	0.93	728	0.5	(3.5 ± 0.6) × 10^{-8}	(1.3 ± 0.2) × 10^{-11}	(8.1 ± 1.6) × 10^{-33}	9.5 ± 0.2	16.2 ± 0.3
15	$Si(OH)_2$	Hexyl	1.0 (THF)	1.05	704	0.5	(2.7 ± 0.5) × 10^{-8}	(1.0 ± 0.2) × 10^{-11}	(7.3 ± 1.4) × 10^{-33}	9.2 ± 0.3	12.4 ± 0.3

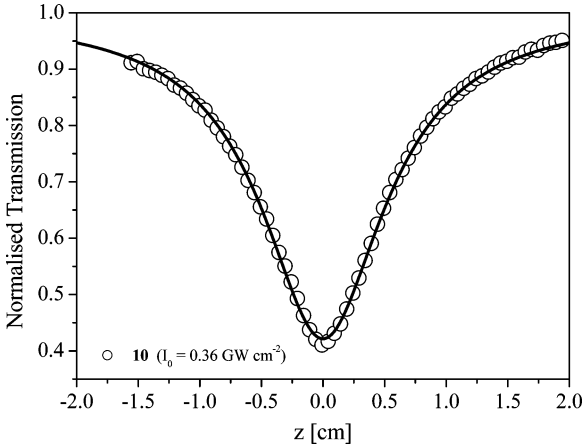

Fig. 2 Typical open-aperture Z-scan spectrum with normalised transmission plotted as a function of sample position, z. Sample curve depicted is for compound **10** under incident focal intensity 0.36 GW cm^{-2}.

of the effective nonlinear absorption coefficient, β_I, against the on-focus beam intensity, I_0, are presented for compounds **1**, **5**, **6**, **9**, **10** and **15** as a sample subset of the entire dataset. Each data point on the plot represents an independent open-aperture Z-scan of the compound in question and the solid lines are sketched merely as guides to the eye. It can clearly be seen that β_I reduces in magnitude with increasing focal intensity I_0 in the plot. The reason for this is probably that the absorption effects are a combination of third and higher odd-order nonlinear absorptions. Despite this, effective third-order nonlinear absorption coefficients, β_I, were estimated by suitably interpolating data similar to those in Fig. 3 for all compounds at on-focus intensities of 0.5 GW cm^{-2} (arbitrarily chosen). Subsequently, using eqn. 3 and 4, effective third-order susceptibilities, Im$\{\chi^{(3)}_{eff}\}$, and molecular second hyperpolarisabilities Im$\{\gamma_{eff}\}$ were calculated for this sample I_0 value. All calculated coefficients are presented in Table 1. The metal-free compounds **1**, **2** and **3** have hexyl, decyl and *iso*-pentyl chains respectively substituted to the macrocycle. The nonlinear absorption coefficient is at its maximum for **1** [(1.8 ± 0.3) × 10^{-8} cm W^{-1}] and minimum for **2** [(1.5 ± 0.3) × 10^{-8} cm W^{-1}], while **2** (decyl substituted) exhibits the largest molecular imaginary hyperpolarisability, with Im$\{\gamma_{eff}\}$ ≈ (4.3 ± 0.8) × 10^{-33} esu. Among the zinc compounds **6**, **7** and **8**, which have hexyl, decyl and *iso*-pentyl chains, respectively,

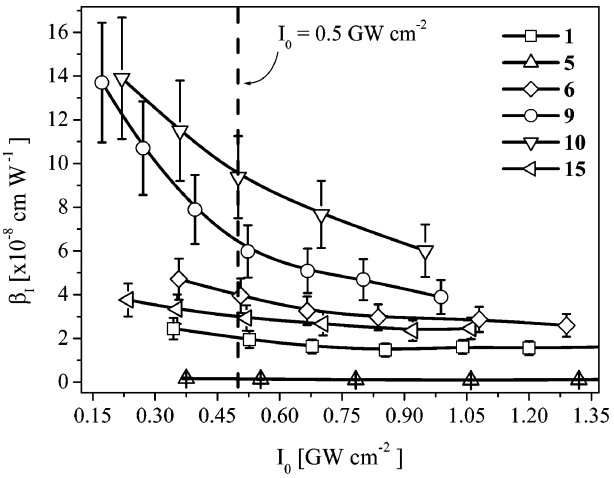

Fig. 3 Plots of effective nonlinear absorption coefficient, β_I, against the on-focus beam intensity, I_0, for compounds **1**, **5**, **6**, **9**, **10** and **15**. Each data point represents an independent open-aperture Z-scan and the solid lines are intended merely as guides to the eye.

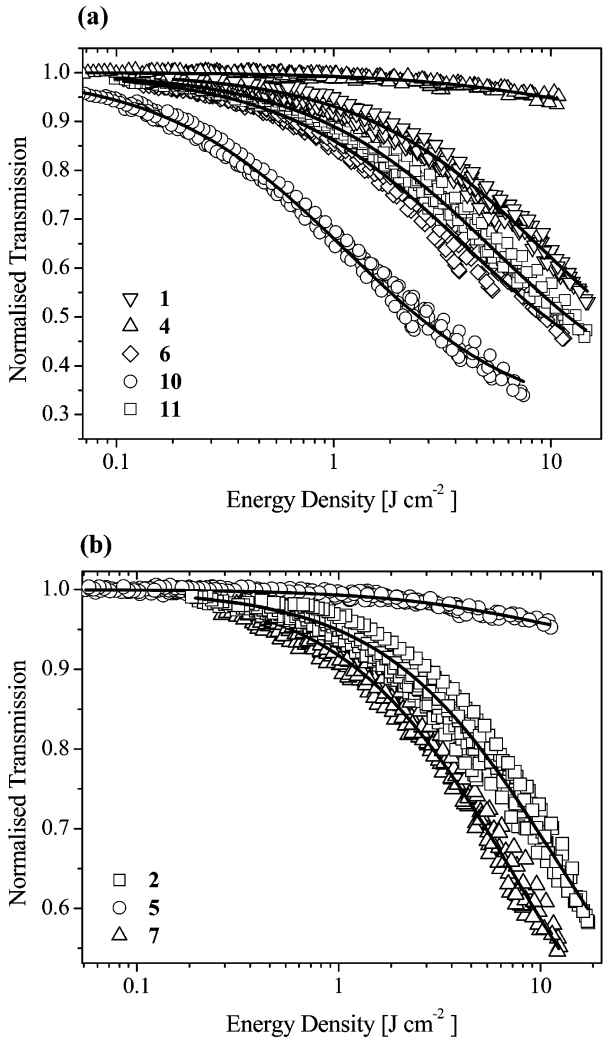

Fig. 4 Plots of normalised transmission against energy density for (a) compounds **1**, **4**, **6**, **10** and **11**, and (b) compounds **2**, **5** and **7**. In the plots, the solid lines are theoretical curve fits used to determine F_{sat} and κ.

substituted to the macrocycle, the decyl-substituted compound **7** exhibits the lowest molecular imaginary hyperpolarisability, with $\mathrm{Im}\{\gamma_{eff}\} \approx (6.9 \pm 1.3) \times 10^{-33}$ esu. For the nickel compounds **4** and **5**, the hexyl-substituted compound (**4**) also exhibits a lower $\mathrm{Im}\{\gamma_{eff}\}$ than its decyl-substituted counterpart (**5**). The Pd-centred compound **10** exhibits the largest nonlinear absorption coefficient in this study, with $\beta_I \approx (9.6 \pm 1.9) \times 10^{-8}$ cm W^{-1}, while the lowest β_I was found for **5**, a Ni complex, with $\beta_I \approx (1.5 \pm 0.3) \times 10^{-9}$ cm W^{-1}. It is worth noting that the magnitude of β_I for the nickel compounds (**4** and **5**) is an order of magnitude or more lower than the β_I values exhibited by any other compound in the study.

The open-aperture spectra were manipulated and plotted as normalised transmission (T_{norm}) against the incident energy density per pulse [$F = \pi w(z)^2$] to further investigate the nonlinear absorption. The nonlinear absorption coefficient, $\alpha(F, F_{sat}, \kappa)$,[27] where $\alpha(F, F_{sat}, \kappa) \approx \alpha_0(1 + F/F_{sat})^{-1}(1 + \kappa F/F_{sat})$, derived from laser rate equations in a static approximation, was used to fit the normalised transmission as a function of this energy density to a superposition of all open-aperture datasets for each compound. In this expression, F represents the energy density, F_{sat} the saturation energy density and κ the ratio of the effective excited- to ground-state absorption cross-sections σ_{ex}/σ_0. The parameters κ (realistically σ_{ex}, as α_0 was measured) and F_{sat} were treated as free constants in the fitting. The α_0, κ and F_{sat} values for each compound are also presented in Table 1.

Representative optical limiting plots are presented in Fig. 4. A subset of the hexyl-substituted compounds (**1**, **4**, **6**, **10** and **11**) are case studied in Fig. 4(a) and a series of decyl-substituted compounds (**2**, **5** and **7**) in Fig. 4(b). The optical limiting of the Pd phthalocyanine **10**, which exhibits the largest β_I at $(9.6 \pm 1.9) \times 10^{-8}$ cm W^{-1}, can be seen in Fig. 4(a). The other four compounds for which data are shown are the metal-free phthalocyanine (**1**) and the Ni (**4**), Zn (**6**) and Pb (**11**) complexes. In terms of the magnitude of the reduction in normalised transmission relative to incident energy density, the palladium compound **10** clearly outperforms the others. It also has a much lower saturation energy density, F_{sat}, than the other phthalocyanines on the plot. Interestingly, the ratio of the absorption cross-sections, κ, is smallest for the Ni phthalocyanine **4** and largest for the Pb phthalocyanine **11**; the κ coefficient for the Pd phthalocyanine is approximately 2.7 times smaller than that for the lead complex and approximately 2.5 times larger than that for the nickel compound. Thus, the κ coefficient of the Pd compound is relatively low, despite it having a larger nonlinear absorption coefficient than compounds **1**, **4** and **6**. This arises because of its relatively large linear absorption coefficient, $\alpha_0 \approx 2.6$ cm^{-1}. It is clear then that substituting Ni into the central cavity has nothing but undesirable effects in terms of optical limiting, as the metal-free phthalocyanine **1** clearly has a much larger nonlinear response than the nickel compound. They have comparable F_{sat} values, (18 ± 3) J cm^{-2} for Ni and (16.8 ± 0.6) J cm^{-2} for the metal-free case, but the κ coefficient for the Ni compound is approximately 6 times smaller than that for the metal-free phthalocyanine. The decyl chain-substituted subset presented in Fig. 4(b) includes the metal-free (**2**), Ni (**5**) and Zn (**7**) compounds. Again, it can clearly be seen that the nickel compound (**5**) is far outperformed by its counterparts. Its κ coefficient is approximately 5.5 times smaller than that for the zinc complex (**7**) and 7 times smaller than that for the metal-free compound (**2**). The two indium phthalocyanines, **13** and **14**, both exhibit large values for their κ coefficient (comparable to that for the lead compound **11**) and provide further data which point to the potential of indium compounds in optical limiting.[10]

General trends in the optical limiting data are investigated in Fig. 5. The ratio of excited- to ground-state absorption coefficients, κ, is plotted against the linear absorption coefficient, α_0, in Fig. 5(a), with data from all compounds included. The relationship between κ and α_0 appears to exhibit a clear trend, with the exception of data from the nickel complexes. The solid line, merely intended as a guide for viewing the data, appears to span the data points in an approximate way, with the exception of data from **4** and **5**. The Ni-centred phthalocyanines are poor optical limiters as they do not exhibit large nonlinear absorption coefficients relative to the other compounds. Thus, excluding the Ni compounds, this seems to suggest that the ratio of the effective excited- to ground-state absorption coefficients has a far closer link to the linear absorption coefficient than to the type of substituents in the central cavity or on the periphery of the phthalocyanine macrocycle. A similar plot of the saturation energy density, F_{sat}, against the linear absorption coefficient, α_0, is presented in Fig. 5(b). In this case, the approximate trend mapped out by the sketched solid line again appears to exhibit a general dependence on α_0. It is most interesting that the Ni compounds appear to be in approximate agreement with the trend line in this case. These data appear to suggest that phthalocyanine design for nonlinear optical applications may be inextricably linked to tuning the linear absorption coefficient due to ground to excited singlet-state transitions.

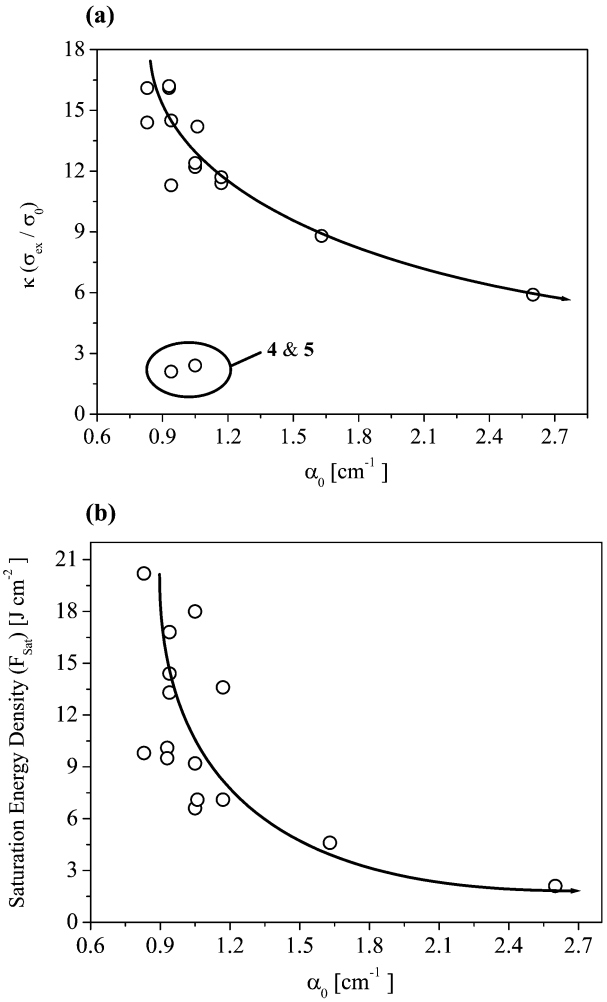

Fig. 5 Investigation of general trends in the optical limiting data: (a) ratio of excited- to ground-state absorption coefficients, κ, plotted against the linear absorption coefficient, α_0, for all compounds; (b) saturation energy density, F_{sat}, plotted against α_0 for all compounds.

4 Conclusion

In summary, a series of 15 unmetallated and metallated octaalkylphthalocyanines have been synthesised and their third-order nonlinear optical properties characterised. The palladium-metallated compound is the strongest nonlinear absorber of the series, but, due to its comparatively high linear absorption coefficient, it exhibits a relatively low ratio of excited- to ground-state absorption cross-sections, κ, when compared to the other compounds. The highest values for κ are exhibited by derivatives metallated with indium and lead. The nickel-metallated compounds are the weakest nonlinear absorbers, indicating their unsuitability as potential materials for practical passive optical limiters. This was interesting in that they were the only compounds to break the apparent trend observed in Fig. 5(a) between κ and the linear absorption coefficient, α_0. Phenomenologically, the data (κ and F_{sat}) were found to follow trends dependent upon α_0. This may have some implications for phthalocyanine design for nonlinear optical applications.

Acknowledgements

This work was supported by CEC contract HPRN-CT2000-00020. We also thank the EPSRC's mass spectrometry service, Swansea, UK, for data for compound characterisation.

References

1 J. W. Perry, K. Mansour, S. R. Marder, K. J. Perry, D. Alvarez and I. Choong, *Opt. Lett.*, 1994, **19**, 625.
2 G. De La Torre, P. Vazquez, F. Agullo-Lopez and T. Torres, *J. Mater. Chem.*, 1998, **8**, 1671.
3 H. S. Nalwa and J. S. Shirk, in *Phthalocyanines: Properties and Applications*, ed. C. C. Leznoff and A. B. P. Lever, VCH Publishers, Inc., New York, 1996, vol. 4, p. 83.
4 C. G. Claessens, W. J. Blau, M. J. Cook, M. Hanack, R. J. M. Nolte and T. Torres, *Monatsh. Chem.*, 2001, **132**, 3.
5 J. Zyss, *Nonlinear Optics: Materials, Physics and Devices*, Academic Press, Boston, 1993.
6 D. S. Chemla and J. Zyss, *Nonlinear Optical Properties of Organic Molecules and Crystals*, Academic Press, Orlando, FL, 1987, vol. 1 and 2.
7 H. S. Nalwa and S. Miyata, *Nonlinear Optics of Organic Molecules and Polymers*, CRC Press, Boca Raton, FL, 1997.
8 J. L. Brédas, C. Adant, P. Tackx, A. Persoons and B. M. Pierce, *Chem. Rev.*, 1994, **94**, 243.
9 D. R. Coulter, V. M. Miskowski, J. W. Perry, T. H. Wei, E. W. van Stryland and D. J. Hagan, *PIE Proc.*, 1989, **1105**, 42.
10 J. S. Shirk, R. G. S. Pong, S. R. Flom, H. Heckmann and M. Hanack, *J. Phys. Chem.*, 2000, **104**, 1438; J. W. Perry, K. Mansour, I. Y. S. Lee, X. L. Wu, P. V. Bedworth, C. T. Chen, D. Ng, S. R. Marder, P. Miles, T. Wada, M. Tian and H. Sasabe, *Science*, 1996, **273**, 1533; M. Hanack and M. Lang, *Adv. Mater.*, 1994, **6**, 819.
11 K. Mansour, D. Alvarez, K. J. Perry, I. Choong, S. R. Marder and J. W. Perry, *Org. Biol. Optoelectron.*, 1993, **1853**, 132; M. K. Casstevens, M. Samoc, J. Pfleger and P. N. Prasad, *J. Chem. Phys.*, 1990, **923**, 2019.
12 M. Hosoda, T. Wada, T. Yamamoto, A. Kaneko, A. F. Garito and H. Sasabe, *Jpn. J. Appl. Phys.*, 1992, **31**, 1071.
13 J. S. Shirk, R. G. S. Pong, F. J. Bartoli and A. W. Snow, *Appl. Phys. Lett.*, 1993, **63**, 1880.
14 F. Z. Henari, A. Davey, W. Blau, P. Haisch and M. Hanack, *J. Porphyrins Phthalocyanines*, 1999, **3**, 331.
15 Y. Chen, Y. L. Song, S. L. Qu and D. Y. Wang, *Opt. Mater.*, 2001, **18**, 219.
16 Y. Chen, L. R. Subramanian, M. Barthel and M. Hanack, *Eur. J. Inorg. Chem.*, 2002, 1032; Y. Chen, M. Barthel, M. Seiler, L. R. Subramanian and M. Hanack, *Angew. Chem.*, 2002, **114**, 3372; Y. Chen, M. Barthel, M. Seiler, L. R. Subramanian and M. Hanack, *Angew. Chem., Int. Ed.*, 2002, **41**, 3239.
17 M. Yamashita, F. Inui, K. Irokawa, A. Morinaga, T. Tako and H. Morawaki, *Appl. Surf. Sci.*, 1998, **883**, 130.
18 T. C. Wen and I. D. Lian, *Synth. Met.*, 1996, **83**, 111.
19 M. J. Cook, *Chem. Record*, 2002, **2**, 225.
20 M. J. Cook, I. Chambrier, S. J. Cracknell, D. A. Mayes and D. A. Russell, *Photochem. Photobiol.*, 1995, **62**, 542.
21 I. Chambrier, M. J. Cook and P. T. Wood, *Chem. Commun.*, 2000, 2133.
22 M. Sheik-Bahae, A. A. Said, T.-H. Wei, D. J. Hagan and E. W. Van Stryland, *IEEE J. Quantum Electron.*, 1990, **26**, 760.
23 N. B. McKeown, I. Chambrier and M. J. Cook, *J. Chem. Soc., Perkin Trans.*, 1990, **1**, 1169.
24 M. J. Cook, S. J. Cracknell and K. J. Harrison, *J. Mater. Chem.*, 1991, **1**, 703.
25 M. Hanack and H. Heckmann, *Eur. J. Chem.*, 1998, 367.
26 M. Aoudia, G. Cheng, V. O. Kennedy, M. E. Kenney and M. A. J. Rodgers, *J. Am. Chem. Soc.*, 1998, **117**, 6029.
27 S. M. O'Flaherty, S. V. Hold, M. J. Cook, T. Torres, Y. Chen, M. Hanack and W. J. Blau, *Adv. Mater.*, 2003, **15**, 19.